

Full Length Article

Experimental and reliability assessment of fire resistance of glue laminated timber beams

Satheeskumar Navaratnam^a, Thisari Munmulla^b, Pathmanthan Rajeev^c,
Thusiyanthan Ponnampalam^d, Solomon Tesfamariam^{e,*}

^a Institute of Innovation, Science and Sustainability (IISS), Federation University Australia, Ballarat, VIC 3353 Australia

^b School of Engineering, RMIT University, Melbourne 3000, Australia

^c Department of Civil & Construction Engineering, Swinburne University of Technology, Australia

^d Ronnie & Koh Consultants Pte Ltd, 573972 Singapore

^e Department of Civil and Environmental Engineering, University of Waterloo, Waterloo, ON N2L 3G1, Canada

ARTICLE INFO

Keywords:

Fire test
Thermal behaviour
GLT beam
Charring rate
Residual stiffness
Deflection under fire

ABSTRACT

Glue-laminated timber (GLT) is an engineered wood product widely used in mass timber construction for its strong structural and fire-resistant properties. However, the fire performance of GLT varies significantly due to the natural and uncertain phenomena (moisture, exposure time, isotropic, homogenous properties, etc.) of fire and timber. This makes it difficult to predict the fire behaviour of the GLT structural elements. To ensure building safety, it is crucial to assess GLT's fire behaviour and post-fire structural integrity during the design stages. This study conducted the experimental tests of GLT beams (280 mm × 560 mm) without loading (1.4 m) and under a four-point bending load (5.4 m). Tests identified thermal behaviour and charring rates of GLT beam. Then, the residual stiffness of the GLT beam was calculated, and the charring rates of the beams were compared with Australian and European standards. Reliability analysis was conducted for beams for a fire exposure of 120 min, considering the charring rates observed through the analysis and simulating the fire insulations. Results show that the charring rate of GLT made with spruce pine timber varied between 0.43 and 0.81 mm/min, with a mean rate of 0.7 mm/min, aligning with both Australian and European standards. However, considering timber density and moisture content, the charring rates in Australian standards were conservative. The study also found that structural capacity significantly degrades under fire, with a 22% reduction in flexural stiffness after 120 min of exposure. Additionally, GLT beams can safely function for 30 min under 75% of their design moment capacity and for 60 min under 50% capacity.

1. Introduction

Timber has become a popular choice due to its sustainability and aesthetics [1,2]. The advent of novel technologies has further encouraged the use of timber, leading to the development of engineered timber products [3,4]. Structural composite lumber (SCL), laminated veneer lumber (LVL), glue-laminated timber (GLT), and cross-laminated timber (CLT) are some engineered timber types used in mid-to-high-rise timber building construction [5–11]. Fire poses a greater threat to timber-based structures and has been a limiting factor in the building height limits [12]. Guidelines are established to use prescriptive methods for timber fire design, which are less complicated but lead to the overdesign of structural elements [13–15]. The use of fire-retardant-treated (FRT) wood, fire-resistant coatings, and the sizing of structural members using the reduced cross-section method are some such procedures used in fire design [16,17].

The natural nature of timber and uncertain phenomena of material and fire behaviour caused significant variations in the structural response to fire [18]. Reliability analysis is suitable for the performance evaluation of structures or elements by understanding the acceptability limits for suitable optimisation procedures [19]. The structural capacity changes with fire, heat flow, and other parameters that can be quantified through experimental tests of existing timber types [20]. Moreover, charring rates can be used in the reliability analysis of timber elements as charring helps to assess the mechanical resistance of timber exposed to fire [21]. The charring rate is an important parameter that most standards use in fire design [22].

Previous research studies evaluate the thermal and mechanical response of GLT beams under fire through medium-scale fire tests [23–25]. Few studies that have considered the temperature variations along the depth of the beams have taken only the thermal properties, where they have either considered the unloaded timber elements or have loaded

* Corresponding author.

E-mail address: Solomon.Tesfamariam@uwaterloo.ca (S. Tesfamariam).
<https://doi.org/10.1016/j.rcns.2025.02.004>

Received 7 November 2024; Received in revised form 12 January 2025; Accepted 23 February 2025

Available online 10 March 2025

2772-7416/© 2025 The Author(s). Published by Elsevier B.V. on behalf of College of Civil Engineering, Tongji University. This is an open access article under the CC BY license (<http://creativecommons.org/licenses/by/4.0/>)

Table 1
The most relevant literature study on GLT subjected to fire.

Size of the specimen (mm × mm × mm)	Area subjected to the fire (mm)	Loading condition	Charring rate (mm/min)	Refs.
150 × 150 × 150	One surface	Unloaded	0.62–0.78	[25]
3800 × 25 × 158	One surface (1000 × 25)	Unloaded	0.63–0.72	[23]
2380 × 100 × 320	One surface (2200 × 100)	Unloaded	0.48–0.73	[27]
1600 × 120 × 120	Pool fire (dia. 250)	Unloaded	0.80	[36]
2000 × 100 × 200	Three surfaces (2000 × 100 (1), 2000 × 200 (2))	Loaded	0.51–0.64	[31]
1330 × 440 × 130	All surfaces except the beam top (1330 × 130)	Unloaded	0.50–0.80	[37]
3660 × 175 × 343	All surfaces except the beam top (3660 × 343)	Unloaded	0.51–0.99	[26]
4700 × 300 × 480	All surfaces except the beam top (4700 × 300)	Loaded	0.52	[38]
250 × 90 × 140	One surface (250 × 140)	Unloaded	0.37–0.71	[39]
6000 × 210 × 420	Three surfaces (4000 × 210(1), 4000 × 420 (2))	Loaded	0.61–0.72	[40]

the burnt timber [21,23,25–27]. Table 1 summarises the past studies of standard fire resistance test on GLT beams. In the studies by Zhang et al. [25] and Hasburgh et al. [26], the effect of service ducts is also taken into consideration. Much research has been focused on the performance of timber and steel-timber connections, either loaded or unloaded [28–30]. Among these tests, some research has been focused on the difference in material properties where different timber species and different local considerations were taken into account [23,31]. In the Fahmi et al. [23] test, a small scale fire test was conducted for a beam of about 3.5 m span where only the centre 1 m length was exposed to fire. The temperature data was collected only at one depth. Mid span deflection and charring rates were identified for different GLT timber grades. Some large-scale fire tests have also evaluated GLT's structural fire performance [32,33]. Xu et al. [32] conducted a large scale compartment fire test to identify the fire propagation and deformation during the fire. However, many studies did not account for temperature flow through GLT beams or temperature variations at different depths, particularly in loaded beams. Additionally, there are few studies on the flexural strength of GLT beams under fire conditions [34,35]. Therefore, further research is needed to understand the thermal properties and fire performance of GLT timber, which vary based on species type and external environmental conditions.

Thus, reliable data is essential for predicting the fire severity and post-fire structural status of GLT beams. This can be achieved through experimental tests and reliability assessments, which can then be used to verify the fire safety and evacuation time for mass-timber buildings. Therefore, current study initially conducted experimental tests to identify the charring rate of the spruce pine GLT beams by measuring temperature variations at different depths and locations during fire exposure. Then, the observed charring rates were used to develop fragility curves for beams under different loading conditions. Additionally, the study monitored the flaming of the beams and the formation and cracking of the char layer at various intervals. Since strength properties are significantly altered during and after fire exposure [41], the deflection variations of the beams under fire were tested. The results are used to derive the residual load-bearing capacity and stiffness of GLT elements. Finally, the experimental data were compared with the standards used in the industry (AS/NZS 1720.4 [42], Eurocode 5 (EC5) [43]) for fire safety.

2. Experimental programmes

Experimental tests on GLT beams were carried out in the horizontal furnace in the commercial fire testing laboratory to understand and analyse the fire performances of GLT. Large scale furnace of 3 m × 6 m area with a height of 3 m was used for the testing where a proportional-integral-derivative controller controlled the furnace temperature. Ceramic fibre insulations were used for the unexposed sides to control heat transfer. Two types of tests were carried out to evaluate the fire performance of the GLT beam. The first one has unloaded GLT beams tested under fire to analyse the heat transfer and charring properties. The second type was a loaded GLT beam tested to understand residual

Table 2
Properties of the timber beams.

Specimen	NLB	LB
Density (kg/m ³)	467 (8%)	474 (8%)
Moisture content	10.3% (9%)	9.3% (10%)
Dimensions (mm) (Width, height, length)	280 × 560 × 1400	280 × 560 × 5400

stiffness. The GLT properties and testing procedures are stated in the following sections.

2.1. Samples detail

The GLT beam (GL24h) is made with fourteen planks of spruce pine, each 40 mm thick and glued together according to EN 14,080 [44]. Melamine formaldehyde glue of density 1226 kgm⁻³ is used as the adhesive. Prior to the tests, the density and moisture contents of beams were measured and detailed in Table 2, and the coefficient of variations (COVs) are given in parentheses. The moisture content was measured at ten locations based on BS EN 13183–3: 2005 [45]. Three test specimens of length 1400 mm with cross-section dimensions of 280 × 560 mm were used in the test on a non-load bearing (NLB) GLT beam.

All three specimens were used in the same furnace test, and the data for each specimen were collected separately. Eleven k-type thermocouples were used for each specimen to capture the temperature variance of the beam during the fire. Thermocouples were installed perpendicularly to the isotherms, considering the convenience of measuring the temperature perpendicular to the heat flow due to the large difference in thermal conductivity between the thermocouple wire and the wood material [46]. The timber beam was longitudinally divided along its span, and precision drilling was performed at designated locations to install thermocouples for temperature monitoring. Subsequently, the two halves were reassembled to restore the beam's integrity. The drilled holes and the beam tops were covered with ceramic fibre insulation to prevent heat transfer through the holes and heat loss through the furnace top. Fig. 1 presents the arrangement of the thermocouples inside the beams. Thermocouples were used at the same location in all the specimens. Points were numbered considering the sample and point numbers (For example, S2-P10 is the 10th point of sample two).

Test specimen (LB) of length 5400 mm with the same cross-section dimensions (280 mm × 560 mm) of the non-load bearing GLT beam was used for the load-bearing test, which was tested under the same prescribed temperature fire curve (refer to Table 1). Since this test only uses one specimen, three sets of data in three locations were introduced for the temperature data collection to validate the experiment. Three data sets of six data points and four data sets with five data points, making a total of thirty-eight data points, as shown in Fig. 2, were used in the test. Fig. 2(a) presents the full side view showing three locations where locations 02 and 03 have all the data sets, and location 01 has only the data set 01. The data sets are numbered in a way such that data sets 01, 02 and 03 have consecutive numbers in each location. Numbers

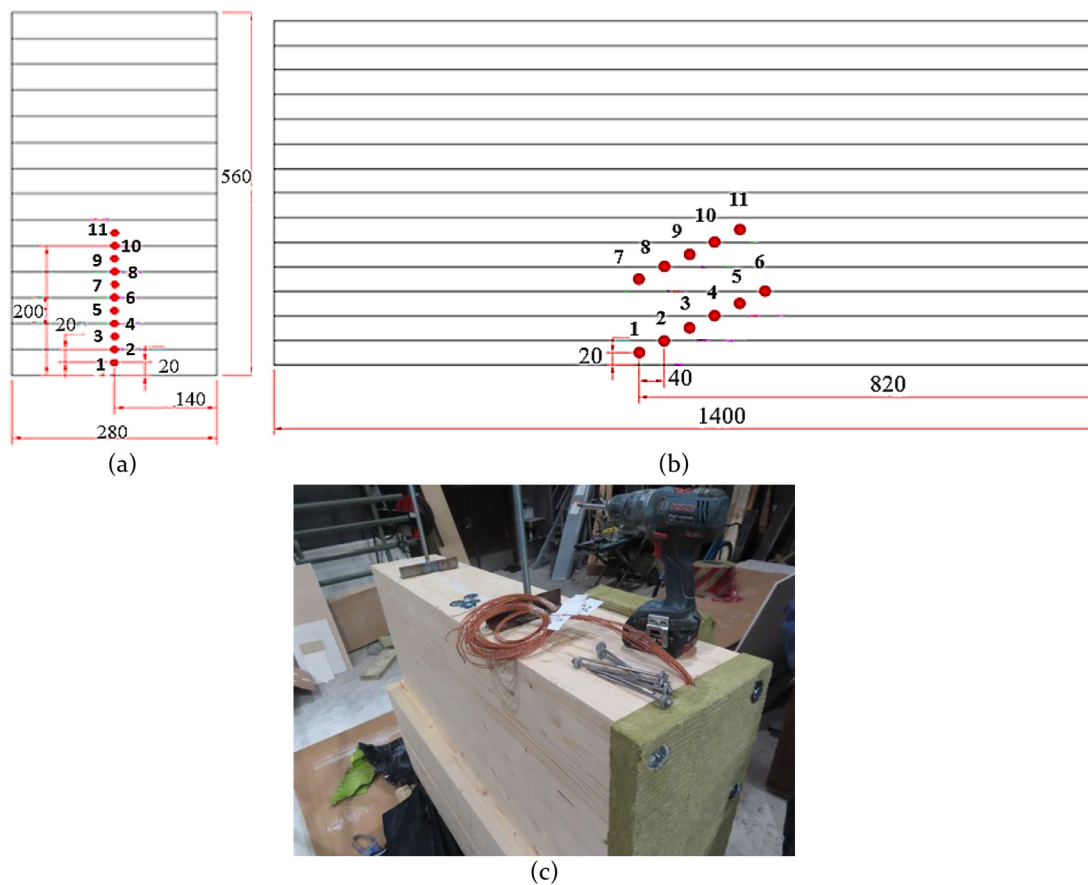


Fig. 1. Location of thermocouples for NLB: (a) Cross-sectional view; (b) Side view, and (c) Manufactured NLB beam.

1 to 6 are occupied by location 01 data set 01. Numbers 7–11 and 12–16 are occupied by data sets 02 and 03, respectively, where each set is numbered from left to right. Hence, point number L3-P15 represents the location 03, and point number is 15, which also indicates that the point belongs to data set 03. Fig. 2(b) presents the cross-sectional view of the thermocouples points, while Fig. 2(c) presents an enlarged side view of location 03. Fig. 2(d) shows the manufactured beam with thermocouples.

2.2. Test details

The fire test was carried out according to EN 1365-3:2002 [47]. The fire test was determined by considering the room geometry, fuel loads, and fire characteristics. ISO 834 [48] standard fire curve was selected and used in the experimental tests represented by Eq. (1), where T represents the temperature and t is the fire exposure time. Two types of tests were performed in this study. The tests for NLB were subjected to standard fire, and the test for LB was subjected to a four-point bending load and standard fire. All three NLB specimens were hung from the ceiling of the furnace and exposed to fire on the bottom sides and vertical edges. Fig. 3 presents the test arrangements of the three specimens. The specimens were not conditioned as they were stored in a test hall from assembly to testing. At the beginning of the test, the room's ambient temperature was 17 °C. After the installation of the specimens in the furnace, the test was continued for 120 min 40 s and terminated.

$$T = 20 + 345 \times \log(8t + 1) \quad (1)$$

For the LB test, the specimen was supported from the short edges, making a clear span of 5200 mm, and the long edges were free to deflect. The bottom side of the beam and the vertical sides parallel to the beam axis were exposed to fire. The LB was loaded with two-point

loads, each at 1833 mm from the beam end (Fig. 4(c)). Each point load was 50 kN, attained by weighing steel weights supported by hydraulic jacks. Fig. 4(a) shows the inside of the furnace and the positioning of the specimen, and Fig. 4(b) shows the loading arrangement in the laboratory. The specimen was not conditioned and stored in the test hall from the assembly to the testing date. At the beginning of the test, the room's ambient temperature was 17 °C. The fire test was continued for 120 min 30 s and terminated. Throughout the test procedures outlined in the European standards EN 13,501–2:2016 [49], complemented with EN 1365–3:2002 [50] and EN 1363–1:2020 [13] were followed.

3. Results and discussions

3.1. Non-load bearing GLT beam (NLB)

Temperature data from the thermocouples and the furnace in NLB testing were extracted to analyse the temperature of the test specimen and the charring. Fig. 5(a) shows the mean temperature of the furnace during the testing, while Fig. 5(b) presents the pressure difference between the furnace and the test hall. Furnace pressure was monitored to ensure accurate and reliable fire test results and to assess the ability of test elements to withstand high temperatures. According to Fig. 5(a), it is evident that mean furnace temperature follows the standard fire curve, simulating similar behaviour under the standard fire. Fig. 5(b) shows that for up to 10 min (678 °C), the pressure inside the furnace oscillates around, increasing and decreasing than the pressure inside the room due to gasses burnt and released. After that, the pressure inside the furnace stabilises with only smaller variations.

The fire exposure of the beams and the combustion under fire with time was captured to visualise the timber performance and appearance.

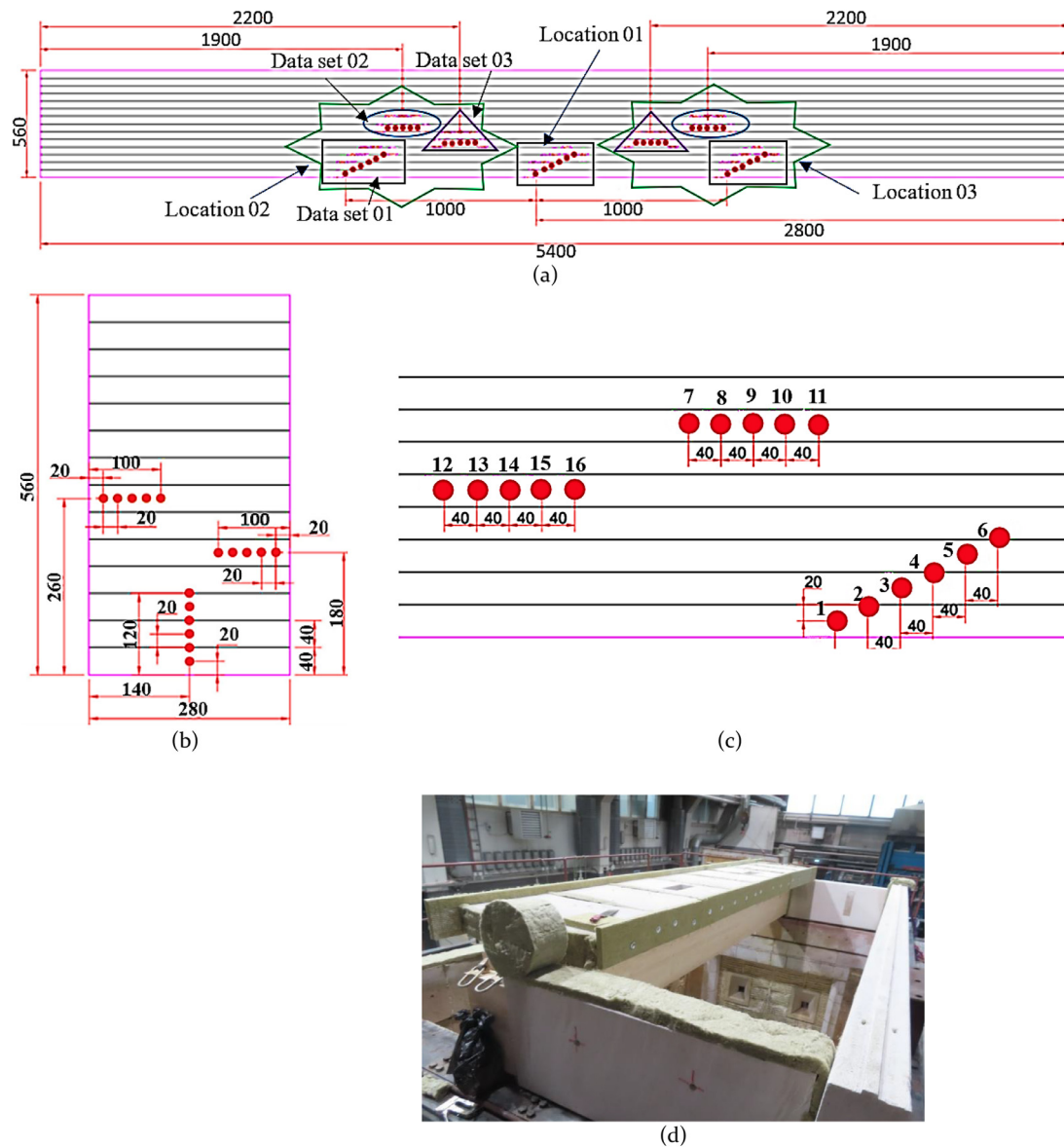


Fig. 2. Location of thermocouples for LB: (a) side view; (b) cross-sectional view; and (c) enlarged side view of location 3; and (d) manufactured LB beam for testing.

Fig. 6 shows the exposed surfaces of the GLT beam in different fire intervals. The beam surfaces start flaming for nearly 2 min time, and at about 22 min, the surface that is charred is cracked, as shown in Fig. 6(a) and (b). The falling of the charred and cracked layers can be seen in Fig. 6(c), which is after 52 min due to natural char dislodgement. Glue line integrity failure was not observed throughout the test, ensuring the 'adhesive's performance under high temperatures. The figures also show the progress of timber fire with large flaming. The capacity of the GLT will be affected by the cooling phase. Therefore, as suggested by Gerney et al. [51] the furnace gas temperature was maintained to follow the linear decrease from the Eurocode parametric fire model at the end and achieved a temperature of about 100 °C in the furnace before the fire was extinguished. The loading was also maintained throughout the period to observe any failures.

Temperature data from 33 thermocouples (i.e., 11 per specimen) were collected. Fig. 7 shows the temperature data from the points of the specimens where point numbers are named after the specimen number and the point number. (La-Pk, a; specimen number, k; point number). According to Fig. 7(a), from point 5 to point 11 (From 100 mm from the bottom), the temperature of the beam is not significantly affected by the

fire. In specimen 01 point 1, which is at 20 mm from the fire surface, it shows a nearly uniform increase in temperature until 940 °C. Then, the increase of temperature decreases, and a nearly stable temperature is obtained, which is around 1015 °C. Considering that the pyrolysis reaction occurs when timber reaches 300 °C, the charring reaches a depth of 20 mm after 45 min of fire exposure. Point 2, which is at 40 mm and at the first glue layer, does not get affected by the fire until about 20 min and then shows a uniform temperature increase, which is nearly 2.7 °C/min. When compared with the temperature increase in point 1, the value is much lesser at first. However, when the temperature at the considered depth reaches a temperature of about 150 °C, the gradient increases up to 28 °C/min, which is even higher than that of point 1. The charring reaches 40 mm depth at nearly 78 min.

When point 3 is compared with the other temperature curves, the behaviour is similar to that of point 2 with lesser temperature gradients. At this point, temperature change occurs after nearly 35 min. Charring reaches 60 mm depth at nearly a time of 97 min. Point 4 also shows a pattern similar to the other points, which reaches a maximum temperature of 300 °C at the end of the test. Other points show significantly lower temperature values, where point 5 reaches a maximum of 60 °C,



Fig. 3. Test setup for NLB: (a) Inside of the furnace; and (b) Test arrangement from outside.

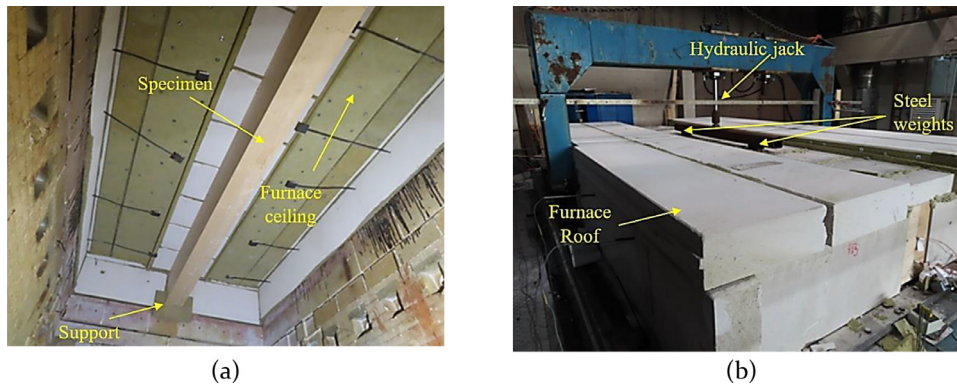


Fig. 4. Test setup for LB: (a) inside of the furnace; and (b) laboratory loading arrangement.

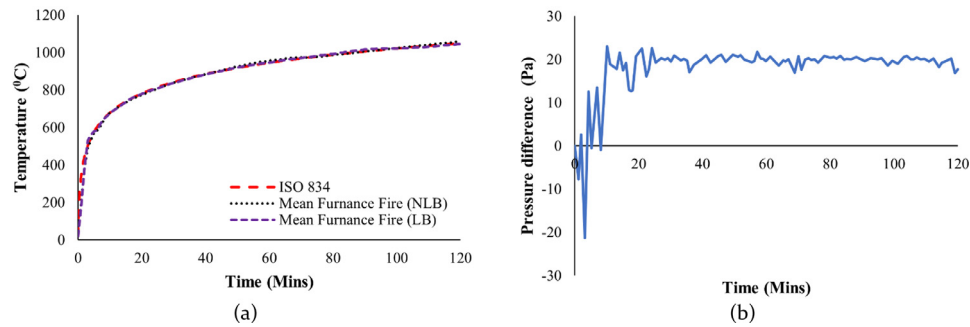


Fig. 5. Experimental data: (a) mean furnace temperature; and (b) the pressure difference between the furnace and the test hall.

and all other points have temperature values less than 20 °C throughout the analysis. Specimen 03 (Fig. 7(c)) also shows a behaviour similar to specimen 01, although the temperature values are not similar due to the variation of timber properties. Temperature data for points 3–6 were not collected due to the malfunction of the thermocouples.

The thermal behaviour of specimen 02 (Fig. 7(b)) shows a deviation from the other specimens, having the temperature of point S2-P2 exceeding point S2-P1 and point S2-P1 experiencing a reduction in temperature at 68 min. This behaviour is due to the malfunctioning of thermocouples. The temperature data gathered from three beams at different depths indicate a uniform increase in temperatures on the surface with time until the surface reaches the furnace temperature. The variations in the temperature gradient in the inner layers were observed at the times when the outer layers reached stable temperatures without temperature rise. This is due to the complete transfer of heat energy to the inner timber layers. These temperature values were also used in calculating the charring rates of the GLT beams (Table 3), considering charring occurs at the time when the timber reaches 300 °C.

Table 3
Charring rate of the experimental specimen NLB.

Depth	Charring rate (mm/min)		
	Specimen 01	Specimen 02	Specimen 03
20	0.45	0.52	0.48
40	0.61	0.55	0.57
60	1.06	1.28	0.78
Final Charring rate	0.71	0.78	0.61
Mean Charring rate	0.7		

Fig. 8 presents cross-sections of the timber beams after the fire test. The beams, which had a depth of 560 mm, have been reduced to 479 mm, 473 mm, and 480 mm in the three specimens. The least uncharred width of the beam at 400 mm is shown by specimen 01, which is 120 mm. At the same time, the maximum is shown by specimen 02, which is about 8% higher. The char rates were calculated at the end of

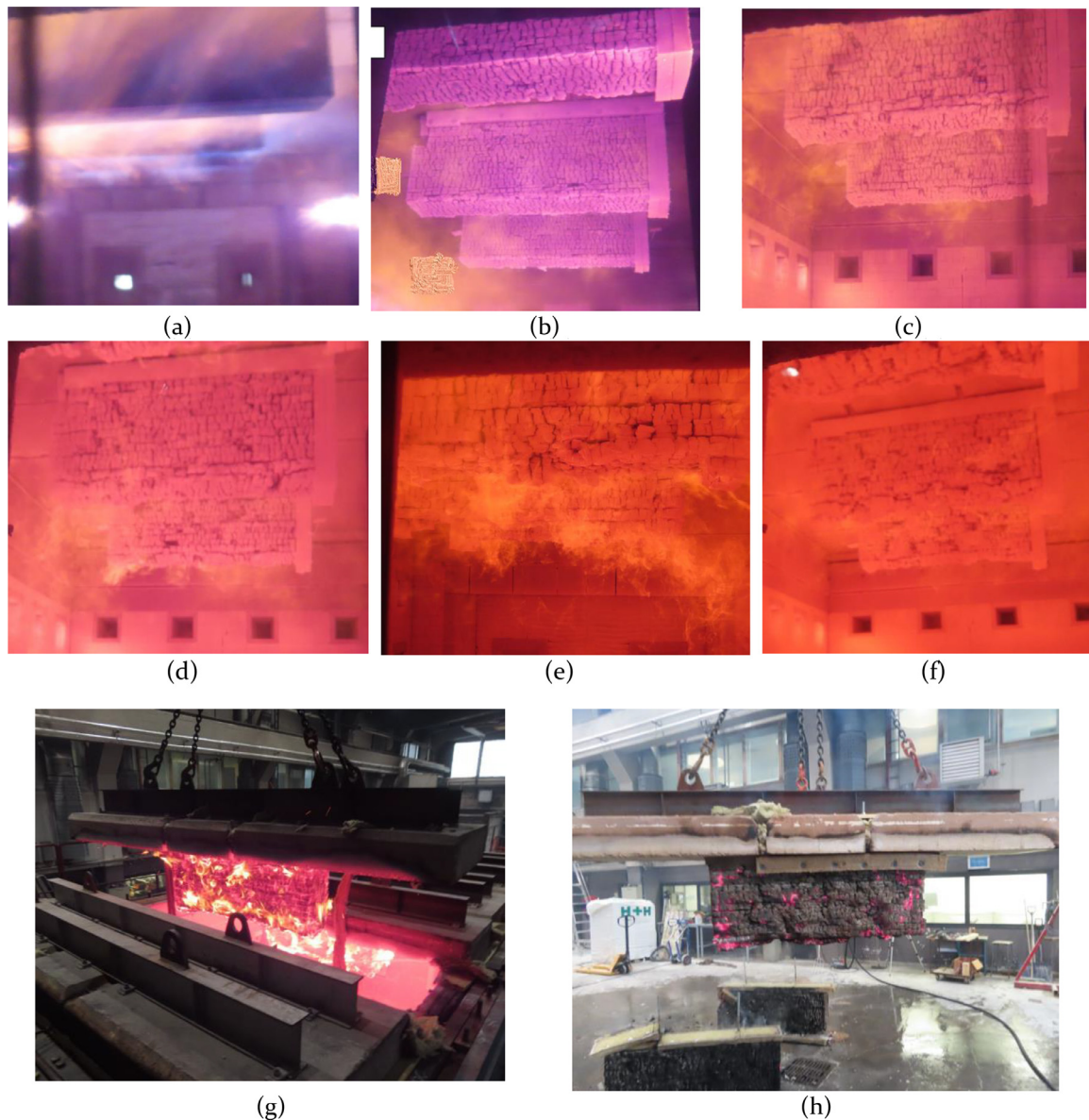


Fig. 6. Fire exposed sides GLT beams at test time (a) 1 min and 50 s; (b) 22 min and 14 s; (c) 52 min and 56 s; (d) 69 min and 10 s; (e) 81 min and 46 s; (f) 115 min and 40 s (g) 1 min and 26 s after the test; and (h) 16 min and 26 s after the test.

Table 4

Charring rate of the NLB specimen according to the char depth at the end of the test.

	Mean char depth along the width (mm)	Charring rate (mm/min)	Mean char depth along the depth (mm)	Charring rate (mm/min)
Specimen 01	74.4	0.62	81.0	0.67
Specimen 02	71.1	0.59	87.0	0.73
Specimen 03	73.1	0.61	80.0	0.67
Mean Charring rate		0.61		0.69

the test from the measured average char depths. The measured average charring rates along the width and the depths are presented in Table 4. Charring rates along the depth are higher than those along the width. This is mainly because of high temperature from the sides of the beam and due to the smaller beam width.

Identifying the reliability of GLT beams in fire will help in identifying the failure time of the beam. Moreover, this would be beneficial in identifying the reliability of complete structures in fire and for fire safety planning (Evacuations). Therefore, the reliability of timber beams based

on charring was calculated. The calculation was done for different load ratios of the beam and different beam dimensions. The design moment capacity (M_d) of NLB beams was calculated according to AS/NZS 1720.4 [42]. Reliability analysis for the timber beams under fire for 120 min was calculated using the Monte Carlo simulation technique [52,53]. The probability of failure (P_F) was calculated as per Eq. (2) where P_F is the standard normal cumulative distribution function (Φ) of the Z-score (Z) of the safety margin (M) of the connection (Eq. (3)). Z is the difference of M to the mean of the M (μ_M) divided by the standard deviation of M

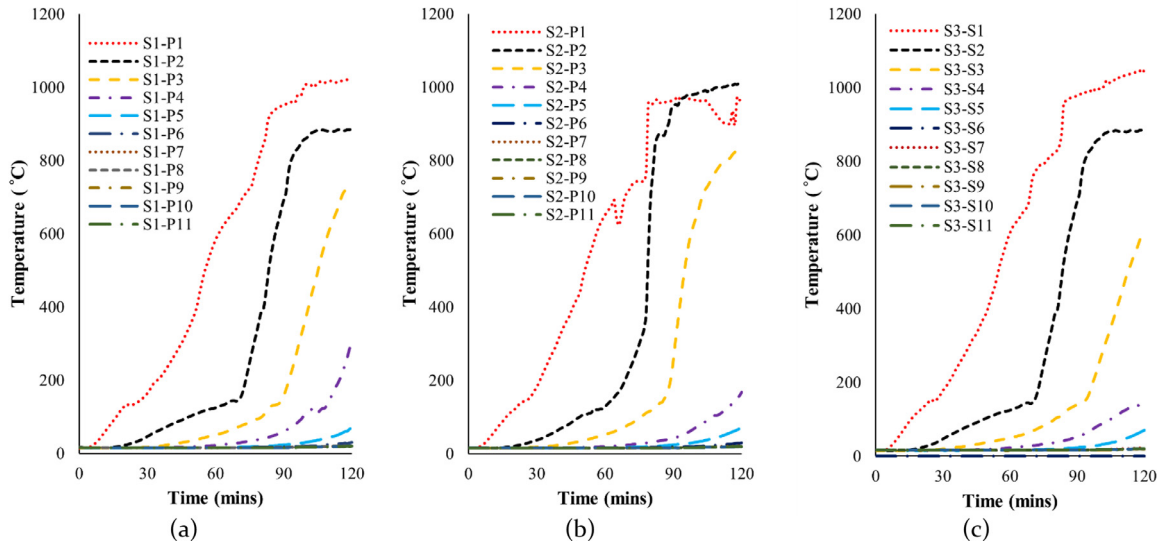


Fig. 7. Temperature curves with time for: (a) Specimen 01; (b) Specimen 02; and (c) Specimen 03.

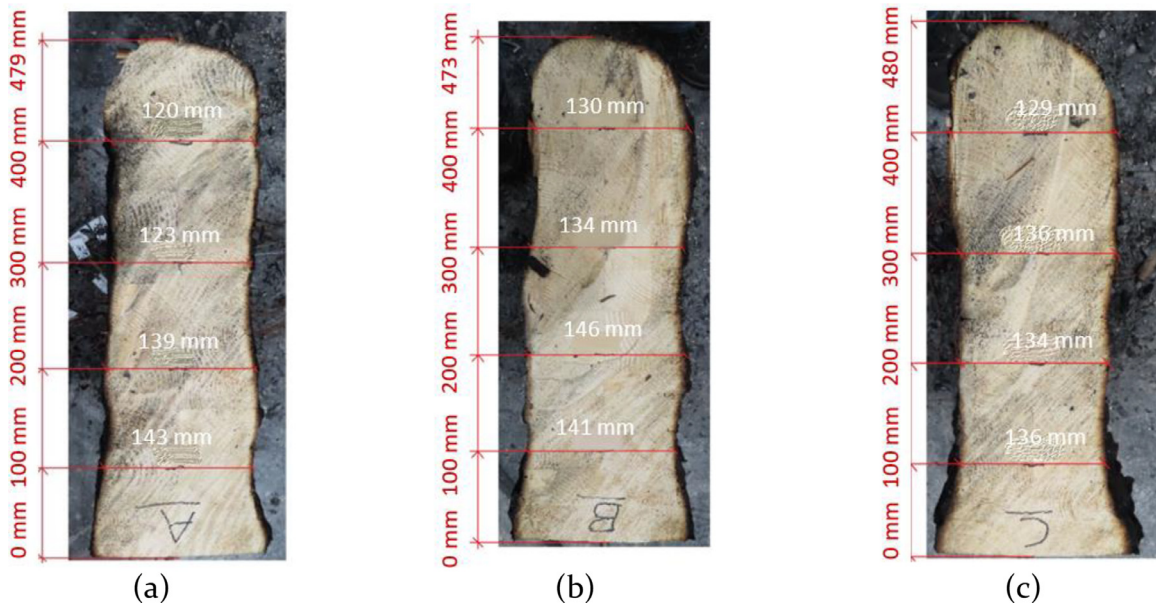


Fig. 8. Cross sections of the specimens after fire: (a) Specimen 01; (b) Specimen 02; and (c) Specimen 03.

(σ_M) . M is the difference in capacity (C) and demand(D) (Eq. (4)).

$$P_F = \phi(Z) \tag{2}$$

$$Z = \frac{(M - \mu_M)}{\sigma_M} \tag{3}$$

$$M = C - D \tag{4}$$

Fig. 9(a) shows the reliability curves developed for the tested beams. Four loading configurations were considered for the analysis, where beams were loaded to achieve 100%, 75%, 50% and 25% of the design moment capacity at room temperature. Later, considering the same charring rates, analysis was developed for different cross sections. Fig. 9(b) shows the reliability curves for different beam depths where the width is maintained the same as in the experiment. In the legends, the letters A, B, C and D denote different beam depths of 560 mm, 480 mm, 400 mm and 360 mm, respectively. The numbers following the letter represent the percentage of the design moment capacity in which the beam is loaded. It is evident that changing cross sections from 560 mm

to 360 mm will nearly reduce 10 min of fire resistance of the beams in any loading percentage. The results also show that considered beam cross sections will fail immediately at any fire event when it is loaded to its maximum capacity. Up to 30- and 70 min fire resistance is observed when the beam is loaded to $M_d = 75\%$ and 50% , respectively. Fig. 9(c) shows reliability curves for different beam widths where the depth is maintained the same. Letters X and Y in Fig. 9(c) were used to represent beam widths of 200 mm and 160 mm, respectively. Although beam widths have less influence on M_d , a high influence on fire resisting time was observed when changing the beam depths. This is mainly due to lesser beam widths when compared with depth and fire exposure from both sides, which results in a higher loss of beam capacity and reliability. According to the results, beams of widths 280 mm with depth ranging from 360 to 560 mm loaded to reach $M_d = 75\%$ can withstand a fire event of 30 min, and beams loaded to 50% can withstand a fire event of 1 h without any failure. Therefore, it is evident that conservative design using beams of larger section sizes, allowing timber to get charred in the event of a fire, is possible. In such events, the remaining

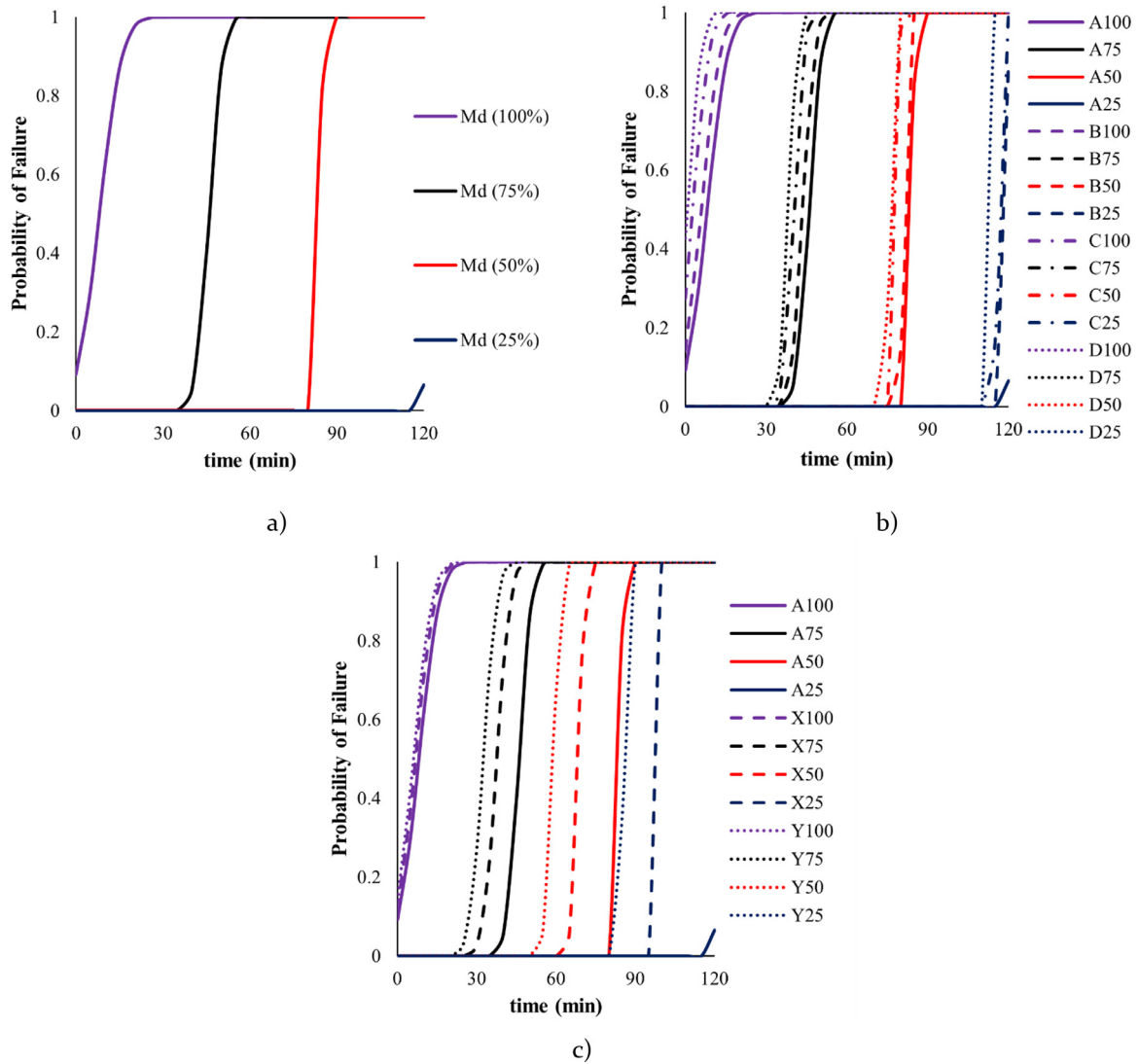


Fig. 9. Probability of failure with fire exposure time for: (a) Beams of cross section 560 mm × 280 mm; (b) Beams with different depths; and (c) Beams with different widths.

beam section will then perform to its maximum capacity, carrying the design load. However, this method is not efficient in terms of material, cost, and space-saving since its timber requires extra material and roof space. On the contrary, using fire protection to reduce the charring rate is a better option.

Fig. 10 shows the reliability analysis of the sample beam section of 560 mm × 480 mm under different fire insulation conditions. To simulate the fire insulation, different charring rates were used for the analysis. Charring rates of 0.3 mm/min to 0.7 mm/min were used for the comparison, and beams were assumed to be loaded to 75% of their bending capacity. According to Fig. 10, with 0.7 mm/min charring rate (CR), fire exposure of 15 min will result in a 25 % probability of failure, whereas for CR=0.6, for 15 min, the failure probability is 0%. Moreover, with CR=0.5, the fire exposure should be more than 30 min to reach the probability of failure of 25%, while CR=0.4 and CR=0.3 can withstand a fire exposure of 45 min and 120 min before exceeding the 25% probability of failure. The failure of the timber beam of CR=0.7, 0.6, 0.5, 0.4 and 0.3 will occur at the fire exposure times of 30 min, 35 min, 40min, 50 min and 65 min. This analysis highlights the critical role of fire insulation for timber and underscores the need for further research to investigate the behavior of insulated timber under fire conditions. Understanding the reliability of GLT beams during fire

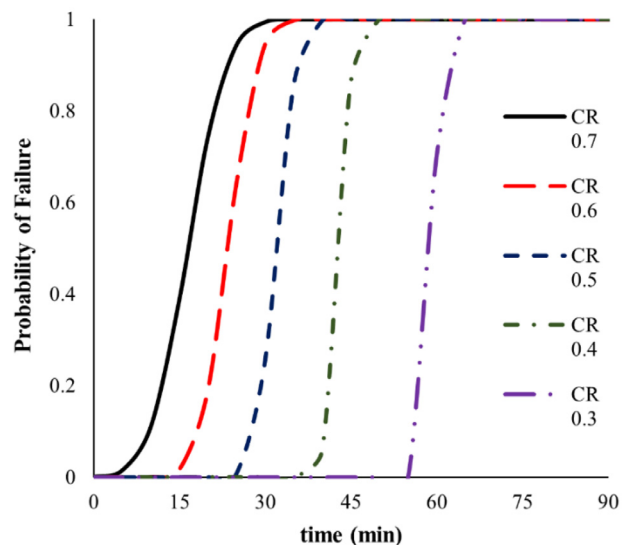


Fig. 10. Probability of failure with fire exposure time for different charring rates.

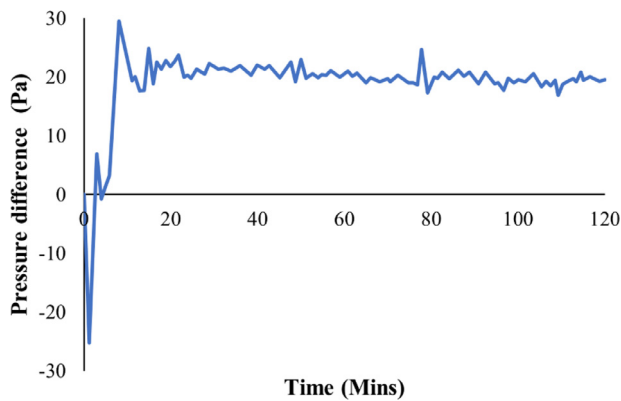


Fig. 11. The pressure difference between the furnace and the test hall.

events is essential for ensuring structural safety and optimising design. This involves examining charring rates, assessing residual mechanical properties, and applying probabilistic methods to address uncertainties. Consequently, these insights will contribute to the development of safer and more efficient structural designs capable of withstanding fire exposure.

3.2. Load-bearing GLT beam (LB)

The test data for the 38 thermocouples were extracted to analyse the temperature variation in the specimen and the charring. The mean temperature of the furnace (Fig. 11(a)) during the LB beam validates that the temperature inside the furnace matches the standard fire curve. Fig. 11 presents the pressure difference between the furnace and the test hall which helps in monitoring and ensuring accurate and reliable fire test results. When compared with the NLB testing, pressure in LB also stabilises to a similar range of pressure. The difference in pressure between the two tests can be seen in the first phase of testing, which is up to 10 min. When compared with NLB, LB shows fewer oscillations where the range of oscillating (–25 to 30) is greater than that of NLB (–21 to 23).

Temperature data from 38 thermocouples were collected. Fig. 12(a) shows the temperature data of data set 01. For a clear representation, only the temperature curves of the three highest temperature points were represented in the figure. When the data location 01 is considered, points L1-P1 and L3-P1, which coincide with each other, and point L2-P1 show the highest temperature variations. For the considered points and location one, the bottommost point L1-P3 (20 mm depth from bottom) receives the highest heat, then the next point L1-P2, which is 40 mm depth, and the least heat is received by L1-P3. The maximum temperature recorded at these points was 982 °C, 912 °C, and 720 °C. The second location deviates from the pattern, making the point at the 40 mm depth from the beam bottom L2-P2 have a similar temperature as the point L2-P1 at 20 mm depth at the end of the test. The highest temperatures recorded at the points L2-P1, L2-P2, and L2-P3 are 1026 °C, 1026 °C, and 817 °C.

Similarly, the third location also shows some deviation from the regular behaviour, having a second point L3-P2 exceeding the temperature of the first point L3-P1 from 85th min to 110th min, having a maximum temperature of 982 °C. For the 2nd and 3rd locations, the first points of each data set 02 and 03 (L2-P7 and L2-P12) in location 2 show errors due to malfunctioning of thermocouples. Therefore, to analyse the lateral temperature behaviour of the horizontally distributed points, temperature data from location 03 were used. Fig. 12(b) presents the temperature behaviour of points in data set 02, while Fig. 12(c) presents the data in data set 03. Both the data sets show a similar variation of temperatures. In both locations up to 40 mm depth,

the effect of fire on temperature increase is higher where the temperature of points L3-P7 reaches 874 °C, and L3-P12 reaches 825 °C while the temperature of points 3–8 and L3-P13 reaches 481 °C and 504 °C. The temperature of points at other depths does not reach the pyrolysis temperature. The figures show a higher temperature gradient in points 1–6, indicating a higher heat transfer rate along the depth than along the width of the beams because of fire on the sides of the beam. These temperature values were also used for charring rate calculations of the GLT beams, considering charring occurs at the time when the timber reaches 300 °C.

The deflection of the beam due to loading under fire was also measured. Fig. 13 shows the deflection at the mid-span during the test. The displacement at the end of loading (15 min) without fire was recorded as 7 mm. The displacement shows a rapid value increment from about the 76th min. The mid-point deflection increased by 25 mm during the fire of 120 min, where the total deflection was 32.5 mm. The average beam depth and width at the end of the 2 h fire are 480 mm and 127 mm. The theoretical increase in deflection during the fire is 26.2 mm. The beam deflection does not exceed either the serviceability limit state (SLS) deflection of 34.6 mm ($L/150$) or the allowable limiting deflection of 121 mm ($L^2/400d$), making the beam fall within the standards followed [54]. The deflection rate was also in the satisfactory range, where the observed maximum deflection rate of 1 mm/min was less than the allowable value of 5.4 mm/min. A similar study conducted by [38] also finds similar beam behaviour under fire.

Table 5 presents the charring rates of the timber specimens in the three locations of the three data sets at a depth of 20 mm, 40 mm, 60 mm and 80 mm. It is evident from the results that charring from the sides in the lateral direction is lesser than the charring from the bottom surface, which is because of the temperature from the sides of the beam and due to the smaller beam width. The maximum charring in locations 02 and 03 is only 0.56 mm/min in data set 03 in location 01, while the minimum of 0.35 mm/min records in data set 02 in location 02. In data set 01, the maximum charring rate of 1.29 mm/min is observed in location 02 at a depth of 60 mm, while a minimum of 0.43 mm/min is also observed in the same location at a depth of 40 mm. In data set 01, location 01 shows a similar charring rate with a mean charring rate of 0.55 mm/min. The second location shows the highest deviation of the values from the lowest to the highest while having a mean charring rate of 0.81 mm/min, which is nearly 47% higher than the charring rate of location 01. Location 03 also shows higher charring rates, where the highest in the location is 1.03 mm/min observed in a depth of 80 mm. The mean charring rate at location 03 is 0.77 mm/min. The higher temperature values observed in locations 02 and 03, near the beam's loaded points, also record the highest charring rates among other locations. Compared with the charring rates in EN 1995-1-2 [14], except for two locations, all other locations fall below the specified charring rate of 0.7 mm/min. Locations 02 and 03 of data set 01 were observed to have 16% and 10% higher rates than the stated values.

Fig. 14 shows the LB GLT beam under fire in different times. Like the NLB beam flaming of the beam, cracking and falling off of the charred layer can be seen, and it is shown in Fig. 14(a)–(f). Fig. 14(g) presents cross-sections in the middle of the timber beams after the fire test. The beam depth has reduced to 480 mm, which is a 14% reduction. A width of 138 mm is observed at the 300 mm depth. A reduced width of 110 mm is observed at 200 mm. It is evident that, despite having the same cross-sectional dimensions, beam LB has a much more reduced cross-sectional area than beam NLB. The char rates were calculated at the end of the test from the measured average char depths. The measured average charring rate along the width is 0.64 mm/min, which is less than the calculated values from the thermocouples' readings but in the permissible range. The change in these values is due to non-uniform charred surfaces and widths and due to visual inspection of charred depth considering the change of colour without considering the temperature values.

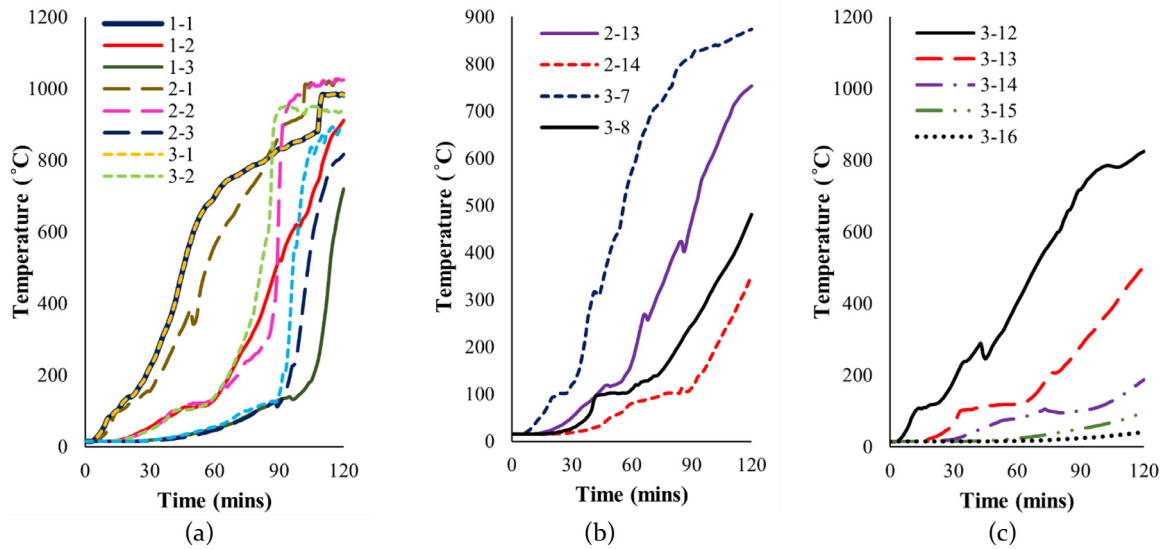


Fig. 12. Temperature curves with time for (a) Location 01; (b) Location 02; and (c) Location 03.

Table 5
Charring rate of the experimental specimen LB.

Depth	Data set 01			Data set 02		Data set 03	
	Location 01 (mm/min)	Location 02 (mm/min)	Location 03 (mm/min)	Location 02 (mm/min)	Location 03 (mm/min)	Location 02 (mm/min)	Location 03 (mm/min)
20	0.56	0.54	0.54	–	0.50	–	0.40
40	0.49	0.43	0.55	0.49	0.35	0.56	0.48
60	0.6	1.29	0.96	–	–	0.47	–
80	–	0.98	1.03	–	–	–	–
Final rate	0.55	0.81	0.77	0.49	0.43	0.4	0.44

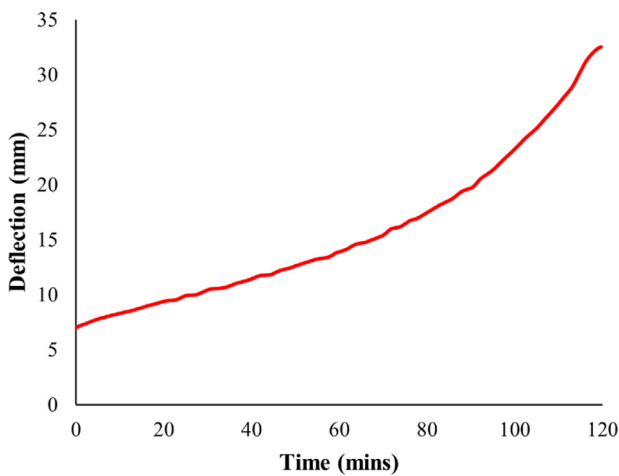


Fig. 13. Mid-span deflection of LB.

3.3. Post-fire residual stiffness and comparison of charring rates with different standards

Evaluating post-fire residual stiffness and comparing charring rates under fire standards like European (EN 1995-1-2), American (ASTM E119), and Australian (AS 1530.4) is critical for assessing the global fire performance of Glulam Timber (GLT). These standards, with distinct temperature-time curves, influence charring rates and thermal degradation, affecting GLT’s mechanical behaviour after fire exposure. Residual stiffness analysis quantifies post-fire load-carrying capacity, complementing charring rate studies to validate safety margins in design

codes. Comparing these results ensures GLT designs meet regional requirements, support the organisation of global standards, and promote the material’s use in fire-resilient structures. This approach enhances fire safety by ensuring reliable performance under diverse fire scenarios.

The experimental data of the LB GLT beam was used to predict post-fire residual flexural stiffness. Since four-point bending was used to load the GLT beam, Eq. (5) can calculate the deflection at the mid-span (P – total load on the beam, L – span of the beam, E – Young’s modulus, I – second moment of area). The equation shows that since the load and the span remain constant, the lowest flexural stiffness (EI) can be obtained as a function of the mid-span deflection, where the highest deflection is observed. The derived flexural stiffness can be used to derive the residual flexural stiffness by reducing the stiffness at room temperature. The modulus of elasticity parallel to grain and perpendicular to grain, shear modulus, compressive and shear strengths of GL24h are 11.6 GPa and 0.39 GPa, 0.69 GPa, 37.5 MPa and 3.85 MPa, respectively (Bedon *et al.* 2020).

$$\Delta y = \frac{23 PL^3}{648 EI} \tag{5}$$

Fig. 15 shows the flexural stiffness of the GLT LB obtained in the experimental during the fire exposure. The flexural stiffnesses were calculated from the beam deflection during the fire. The stiffness calculated represents timber properties due to the temperature variation at the considered time. Therefore, the effect of the heat impacted layer is included in the values. The initial flexural stiffness (at room temperature) obtained in the experimental tests was 35,600 kNm². The flexural stiffness of the GLT beam gradually reduced to 7700 kNm² at the end of the fire test (i.e., 120 min). Fig. 15 also indicates that the residual flexural stiffness of the GLT beam after 120 min of fire exposure is only 22% of its initial flexural stiffness.

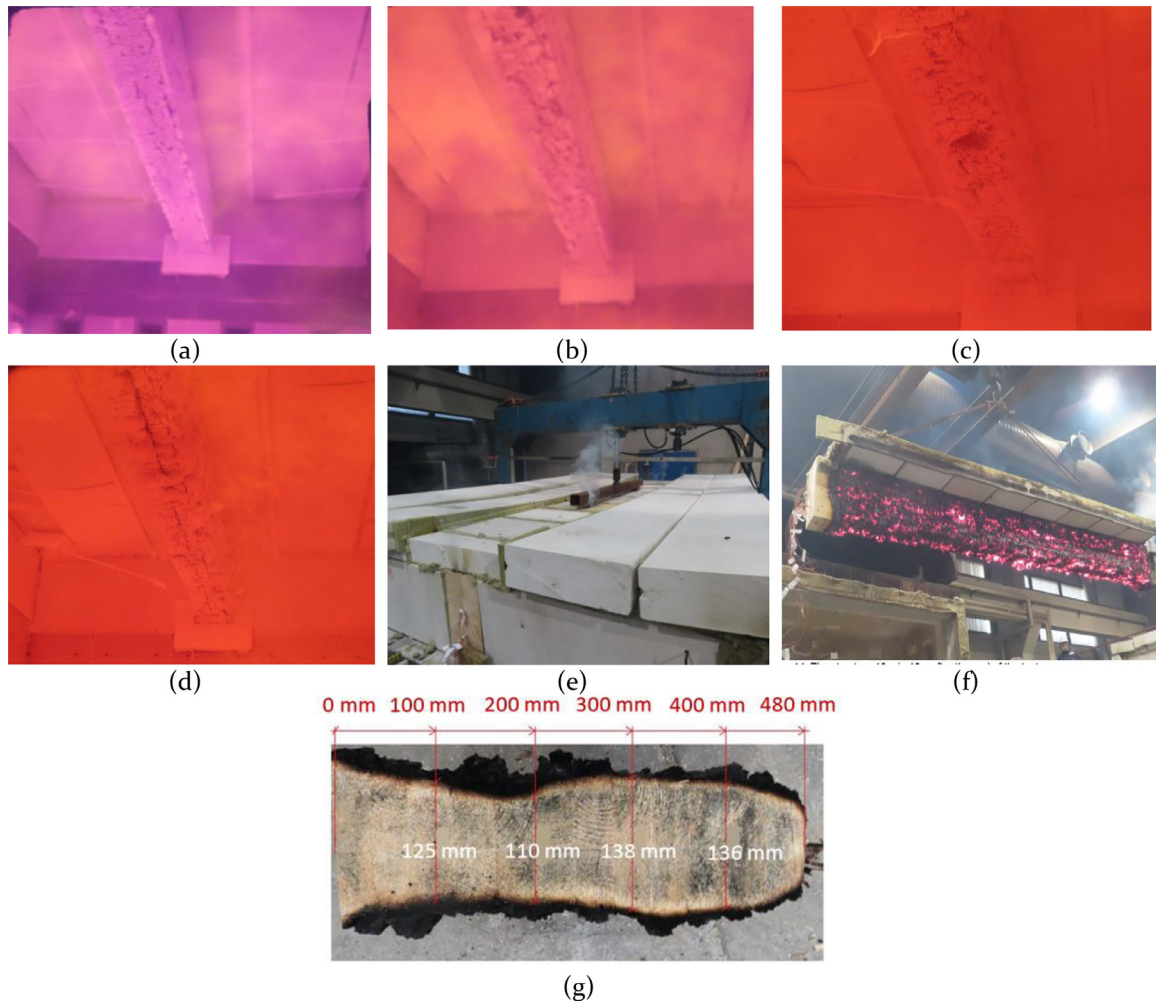


Fig. 14. Fire exposed sides GLT beams at test time (a) 26 min and 18 s; (b) 53 min and 12 s; (c) 87 min and 56 s; (d) 114 min and 30 s; (e) 116 min and 54 s; (f) 11 min and 16 s after the test; and (g) Cross sections of the specimens LB after fire.

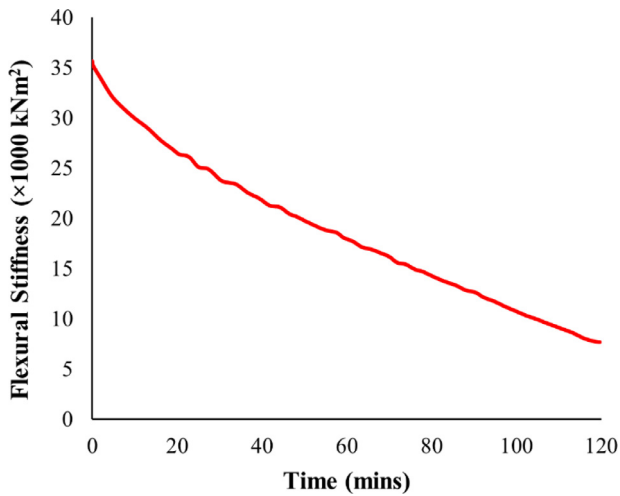


Fig. 15. The flexural stiffness of the GLT beam.

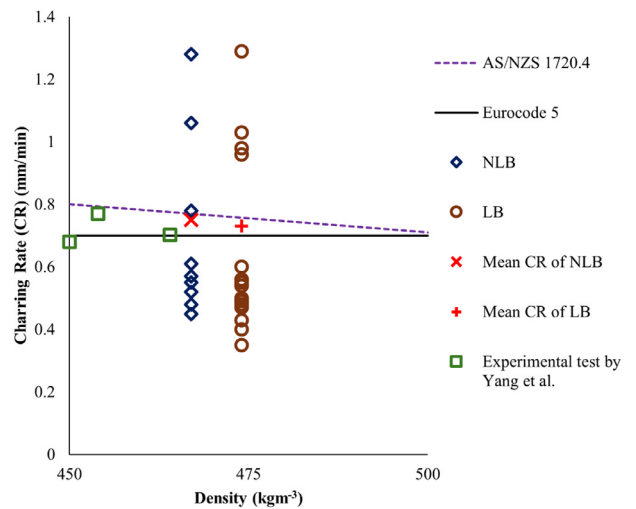


Fig. 16. Comparison of charring rates at different locations in experimental test and the standards.

The charring rates obtained from the experimental tests were compared with the charring rates from different standards and the experimental conducted by Yang et al. [55] for GLT beams with different densities, as presented in Fig. 16. Australian and New Zealand Stan-

dard (AS/NZS 1720.4) [42] and Eurocode 5 (EC5) [43] were used in this comparison. Charring rates according to AS/NZS 1720.4 were calculated considering the densities of the timber with 12% moisture con-

Table 6
Design moment capacity according to Australian Standards.

Parameter	Values for AS/NZS		Values for EC5	
	width	depth	width	depth
Charring rate (c) (mm/min)	0.73		0.70	
Effective depth of charring (d_c) (mm)	94.9		91.0	
Effective dimensions after charring (mm)	width	depth	width	depth
	90.2	465.1	98.0	469.0
ϕ	0.85		–	
k_1	0.97		–	
k_4, k_6, k_9, k_{12}	1		–	
d_0	–		7	
k_0	–		1	
k_m	–		0.7	
t	120		120	
f_b (MPa)	24		24	
Z (mm ³)	3,253,784		3,592,696	
M_d (kN/m)	64		69	

tent. The calculated mean charring rates for NLB and LB GLT beams were 0.75 and 0.73 mm/min. Considering the timber type (softwood) and densities (>290 kg/m³), the charring rate according to Eurocode 5 (EC5) [43] is 0.7 mm/min. The mean of NLB is similar to the Eurocode value, and for LB, the value is slightly higher from 0.01, while AS/NZS 1720.4 [42] gives a conservative value for both cases. The charring rates obtained according to the experimental tests conducted by Yang et al. [55] ranged from 0.68 mm/min to 0.77 mm/min for GLT densities in the range of 450–500 kgm⁻³. According to Fig. 16, charring rates are in a similar range to the standards and experimental results of the study. It can also be seen that all the charring rate values fall under the charring rates suggested by AS/NZS 1720.4 [42], considering the different densities. Fig. 16 shows that the majority of charring rates at different locations in both experiments fall under the values given by the standards, while few exceed them. However, the mean values give similar values as per the standards. The suitability of the standards in fire designs will depend on the circumstances where Eurocode value gives considerably accurate direct value without any property considerations, which saves time, while AS/NZS 1720.4 [42] gives a conservative value with high accuracy, which will differ with the timber properties. Therefore, considering the necessary requirements of the design, either standard can be used.

The theoretical moment capacity (M_d) (Eq. (6)) of the beam according to AS/NZS 1720.4 [42] and Eurocode 5 [14] was calculated considering the charring rate of 0.73 and 0.7. Section modulus (Z) of the effective section after charring was considered for the calculation. For AS/NZS 1720.4 [42], charring depth (d_c) was calculated according to the calculated charring rate (c) (Eqs. (7) and (8)). Beam was assumed to be a primary structural member in structures other than houses with a 5 h effective duration of peak actions. The M_d of the LB beam is 64 kN/m, as presented in Table 6. For the calculations according to the Eurocode, Eqs. (9) and (10) were used, and the values are represented in Table 6.

$$M_d = \phi k_1 k_4 k_6 k_9 k_{12} f'_b Z \quad (6)$$

$$d_c = ct + 7 \text{ mm} \quad (7)$$

$$c = 0.4 + \left(\frac{280}{\delta} \right)^2 \quad (8)$$

$$M_d = k_m f'_b Z \quad (9)$$

$$d_c = ct + k_0 d_0 \quad (10)$$

Table 7 compares the maximum loading allowed on the beam by the AS/NZS 1720.4 [42] and Eurocode 5 according to the results obtained through the experimental tests for four loading configurations. Load calculations according to the Australian Standards and Eurocode were done, taking M_d into consideration, and the measures for experimental tests were done considering the residual flexural stiffness after the fire exposure. According to the results, it can be seen that a more conservative approach was used in AS/NZS 1720.4 [42], where a 30–45 % safety margin was assumed in the calculations. Moreover, the Eurocode values are closer to the experimental values, with a safety margin of 25–41 %.

4. Conclusions

This study presents experimental analyses of grade GL24h GLT beams exposed to ISO-834 standard fire for 120 min. The tests included both non-load-bearing (NLB) and load-bearing (LB) GLT beams, consisting of 14 plies of 40 mm glued together with 0.1 mm of polyurethane adhesive. The experimental results were compared with the charring rates given in the standards. The following conclusions were drawn from the study.

- A charring rate range of 0.43–0.81 mm/min was observed across different locations of the timber beams. The average charring rates were 0.70 mm/min for NLB beams and 0.71 mm/min for LB beams.
- The study also shows that the beams with width of 280 mm and depths ranging from 360 mm to 560 mm, loaded to 75 % of their design moment capacity, can safely function for 30 min in a fire event. Beams loaded to 50 % can withstand a fire event for 60 min without failure.
- Simulating the insulation with changed charring rates, the analysis shows that beams with less charring rates due to insulations, considered beams under a load of 100 kN with reduced charring rates of 0.4 mm/min can withstand fires for 30 min without any failure.
- GLT beams of the considered dimensions (280 mm × 560 mm × 5400 mm) under a four-point bending load of 100 kN can withstand a standard fire for 120 min without any structural failure during the serviceability limit state (SLS). The mid-span deflection is nearly 33.5 mm, which is less than the SLS deflection of 34.6 mm.
- The post-fire residual stiffness of the NLB GLT beam is 7.7 kNm², which is only 22 % of its initial flexural stiffness of 35.6 kNm² after 120 min. This also indicates that an element's structural capacity can be degraded under fire, considering the exposure time.
- The mean charring rate for both beams is similar to the charring rates proposed for GLT beams by EC5, and AS/NZS 1740.2 has conservatively proposed the charring rates considering timber's density and moisture content. Therefore, considering the necessary requirements of the design, either standard can be used where EC5 is simple and efficient, and AS/NZS 1740.2 can be considered as conservative with high reliability on material properties.

Table 7
Maximum permissible loading of GLT beam subjected fire.

	Total permissible load (Pmax)			Percentage difference between	
	Australian Standards (AS/NZS)	European Standards (EC5)	Experimental Results	Experimental and AS/NZS	Experimental and EC5
UDL (kN/m)	19	21	28	32 %	27 %
3-point bending (kN)	50	54	91	46 %	41 %
4-point bending (kN)	74	80	107	31 %	25 %
5-point bending (kN)	74	80	115	35 %	30 %

This research shows the behaviour of GLT under fire and the importance of understanding the behaviour of timber in fire. The study also developed reliability curves for beams with a width of 280 mm and depths ranging from 360 mm to 560 mm. The findings emphasise the need for testing and developing a common framework or model to predict timber behaviour, considering different timber types and species. Future studies should explore the independent effects of modulus of elasticity (E) and moment of inertia (I) on flexural stiffness under fire conditions. This can be achieved by numerical analysis which are validated by the experiments conducted in this study.

Relevance to resilience

This article investigates the performance of glulam timber beams under fire loads, focusing on their structural behaviour and safety. Experimental results are validated numerically, accounting for uncertainties in material properties and fire dynamics. A reliability-based assessment provides critical insights for post-fire downtime, resilience, and recovery planning. The findings support multi-hazard design frameworks that address both fire and earthquake risks, contributing to safer and more robust infrastructure.

Funding statement

This work was funded by the 2022-2023 Fellowship of the Coalition for Disaster Resilient Infrastructure (CDRI), [210927702](#). The authors also acknowledge the funding support from Ronnie & Koh Consultants Pte Ltd, [573972](#) Singapore.

Data availability

The datasets generated during and/or analysed during the current study are not publicly available due to privacy. but are available from the corresponding author upon request.

Symbols	
δ	density
Φ	capacity factor
c	charring rate
d_c	charring depth
f_b	characteristic bending strength
k_1	the factor for load duration
k_4	factor for in-service absorption or desorption of moisture by timber
k_6	factor for temperature/humidity effect
k_9	factor for load sharing in grid system
k_{12}	factor for stability
M_d	design moment capacity
t	Time
Z	section modulus
Abbreviations	
CR	charring rate
FET	fire exposure time
FRT	fire-retardant-treated
GLT	glue-laminated timber
SLS	serviceability limit state
UDL	uniformly distributed load

Declaration of competing interest

The authors declare there are no conflicts of interest in this research.

CRedit authorship contribution statement

Satheeskumar Navaratnam: Writing – original draft, Methodology, Investigation, Formal analysis, Conceptualization. **Thisari Munmulla:** Writing – original draft, Formal analysis, Data curation, Conceptualization. **Pathmanthan Rajeev:** Writing – review & editing, Supervision, Conceptualization. **Thusiyanthan Ponnampalam:** Project administration, Methodology, Investigation. **Solomon Tesfamariam:** Writing – review & editing, Supervision, Conceptualization.

Acknowledgement

The authors acknowledge the Coalition for Disaster Resilient Infrastructure (CDRI), Ronnie & Koh Consultants Pte Ltd, [573972](#) Singapore and RMIT University for their support in terms of financial, and other research facilities.

References

- [1] Ramage MH, Burrige H, Busse-Wicher M, Fereday G, Reynolds T, Shah DU, Wu G, Yu L, Fleming P, Densley-Tingley D, Allwood J. The wood from the trees: the use of timber in construction. *Renew Sustain Energy Rev* 2017;68:333–59.
- [2] Suzuki J-i, Mizukami T, Naruse T, Araki Y. Fire resistance of timber panel structures under standard fire exposure. *Fire Technol* 2016;52:1015–34.
- [3] Bhandari S, Riggio M, Jahedi S, Fischer EC, Muszynski L, Luo Z. A review of modular cross laminated timber construction: implications for temporary housing in seismic areas. *J Build Eng* 2023;63:105485.
- [4] Singh T, Arpanaei A, Elustondo D, Wang Y, Stocchero A, West TA, Fu Q. Emerging technologies for the development of wood products towards extended carbon storage and CO₂ capture. *Carbon Capture Sci Technol* 2022;4:100057.
- [5] Johnson E, Yazdani N. Long-term durability of structural composite lumber in bridge applications. *Transp Res Rec* 2001;1770:149–54.
- [6] Milner HR, Woodard AC. 8 - Sustainability of engineered wood products. In: Khatib JM, editor. *Sustainability of construction materials*. 2nd ed.. Woodhead Publishing; 2016. p. 159–80.
- [7] Šuhajdová E, Schmid P, Novotný M, Pěňčík J, Šuhajda K, Uhlík O. Experimental research on hybrid hardwood glue-laminated beams. *Buildings* 2025;13(4):1055.
- [8] De Araujo V, Christoforo A. The global cross-laminated timber (CLT) industry: a systematic review and a sectoral survey of its main developers. *Sustainability* 2023;15(10):7827.
- [9] Latour M, Rizzano G. Seismic behavior of cross-laminated timber panel buildings equipped with traditional and innovative connectors. *Arch Civ Mech Eng* 2017;17:382–99.
- [10] Zheng X, He M, Li Z, Luo Q. Long-term performance of post-tensioned cross-laminated timber (CLT) shear walls: hygro-mechanical model validation and parametric analysis. *Arch Civ Mech Eng* 2022;22:68.
- [11] van de Lindt JW, Furlley J, Amini MO, Pei S, Tamagnone G, Barbosa AR, Rammer D, Line P, Fragiocomo M, Popovski M. Experimental seismic behavior of a two-story CLT platform building. *Eng Struct* 2019;183:408–22.
- [12] Cheng CH, Chow CL, Yue TK, Ng YW, Chow WK. Smoke hazards of tall timber buildings with new products. *Encyclopedia* 2022:593–601 (Basel, 2021).
- [13] European Standards Organization. ISO 834-10:2020 - fire resistance tests. Part 1: general requirements. Rue de la Science 23, B-1040 Brussels International Standards Organization; 2020.
- [14] European Standards Organization. EN 1995-1-2:2005. Eurocode 5: design of timber structures - part 1-2: general - structural fire design; 2005.
- [15] Australian Building Codes Board. National Construction Code (NCC). Building code of Australia. 2016.
- [16] Dagenais C, Buchanan A, Östman B, Klippel M, Barber D, Claridge E, Dunn A, England P, Janssens M, Just A, Mikkola E. Fire safe use of wood in buildings: Global design guide. In *World Conference on Timber Engineering*, 19-22 June 2023, Oslo, Norway (pp. 4627–35).
- [17] Östman B, Schmid J, Klippel M, Just A, Werther N, Brandon D. Fire design of CLT in Europe. *Wood Fiber Sci* 2018;50(Special Issue):68–82.
- [18] Godoy Dellepiani M, Roa Munoz G, Yanez SJ, Guzmán CF, Saavedra Flores EI, Pina JC. Numerical study of the thermo-mechanical behavior of steel–timber structures exposed to fire. *J Build Eng* 2023:65.
- [19] Yang DY, Teng JG, Frangopol DM. Cross-entropy-based adaptive importance sampling for time-dependent reliability analysis of deteriorating structures. *Struct Saf* 2017;66:38–50.
- [20] Wiesner F, Bisby LA, Bartlett AI, Hidalgo JP, Santamaria S, Deeny S, Hadden RM. Structural capacity in fire of laminated timber elements in compartments with exposed timber surfaces. *Eng Struct* 2019;179:284–95.
- [21] Kucíková L, Janda T, Sýkora J, Šejnoha M, Marseglia G. Experimental and numerical investigation of the response of GLT beams exposed to fire. *Constr Build Mater* 2021;299:123846.
- [22] Qin R, Zhou A, Chow CL, Lau D. Structural performance and charring of loaded wood under fire. *Eng Struct* 2021;228:111491.
- [23] Fahrni R, Klippel M, Just A, Ollino A, Frangi A. Fire tests on glued-laminated timber beams with specific local material properties. *Fire Saf J* 2019;107:161–9.
- [24] Ni Z., Peng L., Qiu P., Zhang H. Experimental study on fire resistance performance of timber assemblies. 2012;45:108–14.
- [25] Zhang Y, Zhang X, Wang L. Experimental validation and simplified design of an energy-based time equivalent method applied to evaluate the fire resistance of the glulam exposed to parametric fire. *Eng Struct* 2022;272:115051.
- [26] Hasburgh L., Bourne K., Barber D. Fire performance of penetrations in glulam beams: a preliminary study. *World Conference on Timber Engineering*. 19-22 June 2023, Oslo, Norway.
- [27] Kucíková L, Janda T, Šejnoha M, Sýkora J. Experimental investigation of fire resistance of GLT beams. *Int. J. Comput. Methods Exp Meas* 2020;8:99–110.
- [28] Shakimon MN, Hassan R, Malek NJ, Zainal A, Awaludin A, Hamid NHA, Lum WC, Salit MS. European yield model exponential decay constant modification for glulam after fire exposure. *Forests* 2022;13(12):2012.

- [29] Luo J, He M, Li Z, Gan Z, Wang X, Liang F. Experimental and numerical investigation into the fire performance of glulam bolted beam-to-column connections under coupled moment and shear force. *J Build Eng* 2022;46.
- [30] Navaratnam S, Thamboo J, Ponnampalam T, Venkatesan S, Chong KB. Mechanical performance of glued-in rod glulam beam to column moment connection: an experimental study. *J Build Eng* 2022;50:104131.
- [31] Tang Z, Yue K, Lu D, Shi X, Chu Y, Tian Z, et al. Experimental investigation into fire performance of mixed species glulam beams under three-side fire exposure. *Eur J Wood Wood Prod* 2022;80:235–45.
- [32] Xu H, Pope I, Gupta V, Cadena J, Carrascal J, Lange D, et al. Large-scale compartment fires to develop a self-extinction design framework for mass timber—Part 1: literature review and methodology. *Fire Saf J* 2022;128:103523.
- [33] Mitchell H, Kotsovinos P, Richter F, Thomson D, Barber D, Rein G. Review of fire experiments in mass timber compartments: current understanding, limitations, and research gaps. *Fire Mater* 2023;47(4):415–32.
- [34] Yang J, Chen J, J-w Zeng, W-y Wang, X-l Zhao. Fire resistance performance of glulam beam. *J Cent South Univ* 2017;24:929–36.
- [35] Verma N, Salem O. Comparative study on the flexural behaviour of glulam built-up beams based on ambient and standard fire tests. *Eng Struct* 2021;233:111759.
- [36] Wei S, Yang H, Gao B, Cheng H, Lu R, Dong L. Experimental research on temperature distribution and charring rate of typical components of wood structure building. *J Fire Sci* 2022;40:134–52.
- [37] Md Daud AF, Ahmad Z, Hassan R. Charring rate of glued laminated timber (Glulam) made from selected Malaysian tropical timber. In: Hassan R, Yusoff M, Alis-ibramulisi A, Mohd Amin N, Ismail Z, editors. InCIEC 2014. Singapore: Springer Singapore; 2015. p. 1107–16.
- [38] C-k Chen, J Yang, Chen J, J-w Zeng, W-y Wang, X-l Zhao. Fire resistance performance of glulam beam. *J Cent South Univ* 2017;24:929–36.
- [39] Njankouo JM, Dotreppe JC, Franssen JM. Experimental study of the charring rate of tropical hardwoods. *Fire Mater* 2004;28:15–24.
- [40] Kinjo H, Hirashima T, Yusa S, Horio T, Matsumoto T. Fire performance, including the cooling phase, of structural glued laminated timber beams. *J Struct Fire Eng* 2016;7:349–64.
- [41] Bai Y, Zhang J, Shen H. Residual compressive load-carrying capacity of cross-laminated timber walls after exposed to one-side fire. *J Build Eng* 2021;34:101931.
- [42] Standards Australia and New Zealand. AS/NZS 1720.4. Timber structures – part 4: fire resistance of timber elements. 2019.
- [43] European Standards Organization. EN 1995-1-1:2004. Eurocode 5: design of timber structures - part 1-1: general - common rules and rules for buildings. 2004.
- [44] British Standards Institution. BS EN 14080. Timber structures — glued laminated timber and glued solid timber — requirements: British Standards Institution (BSI); 2014.
- [45] European Standards Organization. BS EN 13183-3: 2005 moisture content of a piece of sawn timber - Part 3: estimation by capacitance method: Ente Nazionale Italiano Di Unificazione (UNI); 2005.
- [46] Fahrni R., Schmid J., Klippel M., Frangi A. Correct temperature measurements in fire exposed wood. World Conference on Timber Engineering. Seoul, South Korea: ETH Library; 2018.
- [47] European Standards Organization. EN 1365-3: 2002. Fire resistance tests for load-bearing elements-beams Ente Nazionale Italiano di Unificazione (UNI); 2001.
- [48] European Standards Organization. Fire resistance tests part 1: general requirements. Rue de la science 23, B-1040 Brussels CEN-CENELEC management centre; 2020.
- [49] European Standards Organization. EN 13501-2:2016. Fire classification of construction products and building elements part 2: classification using data from fire resistance tests, excluding ventilation services. Avenue marnix 17, B-1000 Brussels CEN-CENELEC management centre; 2016.
- [50] European Standards Organization. EN 1365-3: 2002. Fire resistance tests for load-bearing elements-beams Ente Nazionale Italiano Di Unificazione (UNI); 2002.
- [51] Gernay T, Franssen JM, Robert F, McNamee R, Felicetti R, Bamonte P, Brunkhorst S, Mohaine S, Zehfuß J. Experimental investigation of structural failure during the cooling phase of a fire: concrete columns. *Fire Saf J* 2022;134:103691.
- [52] Zou T., Mourelatos Z.P., Mahadevan S. Reliability analysis using Monte Carlo Simulation and response surface methods. *SAE Transactions*. 2004;113:140–7.
- [53] Lin W, Su C. An efficient Monte-Carlo simulation for the dynamic reliability analysis of jacket platforms subjected to random wave loads. *J Mar Sci Eng* 2021;9(4):380.
- [54] European Standards Organization. BS EN 1365-2:2014 fire resistance tests for load-bearing elements floors and roofs. 2014.
- [55] Yang TH, Wang SY, Tsai MJ, Lin CY. The charring depth and charring rate of glued laminated timber after a standard fire exposure test. *Build Environ* 2009;44:231–6.